Assessment of rock glaciers, water storage, and permafrost distribution in Guokalariju, Tibetan Plateau

Mengzhen Li, Yanmin Yang, Zhaoyu Peng, Gengnian Liu

College of Urban and Environmental Sciences, Peking University, Beijing, 100871, China

5   *Correspondence to*: Gengnian Liu (liugn@pku.edu.cn)

Abstract. Rock glaciers are important hydrological reserves in arid and semi-arid regions. Rock glaciers' activity states can indicate the existence of permafrost. To help explore further the development mechanisms of rock glaciers in semi-arid and humid transition regions, this paper provides a detailed rock glacier inventory of the Guokalariju (GKLRJ) area of the Tibetan Plateau (TP) using a manual visual interpretation of Google Earth Pro

10   remote sensing imagery. We also estimated the water volume equivalent (WVEQ) and the distribution of permafrost probabilities in the GKLRJ for the first time. Approximately 5,053 rock glaciers were identified, covering a total area of ~ 428.71 km^2. Rock glaciers are unevenly distributed within the three sub-regions R1, R2 and R3 from east to west, with 80% of them concentrated in R2, where climatic and topographic conditions are most favorable. Limited by topographic conditions, rock glaciers are more commonly distributed on west-facing

15   aspects (NW and W). When other conditions are met, increases in precipitation are conducive to rock glaciers forming at lower altitudes. Indeed, the lower limit of rock glaciers' mean altitude decreased eastward, with increasing precipitation. Estimates of the water storage capacity of rock glaciers obtained by applying different methods varied considerably, but all showed the potential hydrological value of rock glaciers. The maximum possible water storage in these rock glaciers was 6.82 km^3, or ~ 56% of the local clean ice glacier storage. In R1,

20   where the climate is the driest, the water storage capacity of rock glaciers was estimated to be up to twice as large as that of the sub-region's clean ice glaciers. Permafrost is widespread above ~ 4,476 m above sea level (asl). Our results showed that the regression model, based on the rock glacier inventory, can consistently predict the possible range of modern permafrost. These results may also have some value for regional water resource management, disaster prevention, and sustainable development strategies.

25   **1 Introduction**

Rock glaciers are periglacial landforms often observed above the timberline in alpine mountains. They are formed by rocks and ice that move down a slope, driven by gravity (French, 2007; RGIK, 2021). As striking features of viscous flow in perennially frozen materials, they can reflect permafrost conditions in mountainous areas. Their lowest altitudes are often considered to represent the lower limit of discontinuous regional permafrost

30   occurrence (Giardino and Vitek, 1988; Barsch, 1992, 1996; Barsch, 1996; Kääb *et al.*, 1997; Schmid *et al.*, 2015; Selley *et al.*, 2018; Baral *et al.*, 2019; Hassan *et al.*, 2021); their states (intact or relict) can be used in Permafrost Zonation Index (PZI) models to predict the probability of permafrost occurrence where field observation data are scarce (Cao *et al.*, 2021; Boeckli *et al.*, 2012a). The large-scale distribution of active rock glaciers is influenced by the complex interaction of climatic and topographic factors (Schrott, 1996; Millar and Westfall, 2008; Pandey,

35   2019). Global climate change may affect the stability of rock glaciers and permafrost, thus impacting slope

stability, vegetation coverage, runoff patterns and water quality, with possible consequences for periodic landslides, debris flows, floods and other geological disasters (Barsch, 1996; Schoeneich *et al.*, 2015; Blöthe *et al.*,2019; Hassan *et al.*, 2021). Exploring their spatial distribution and evolution is therefore significant for paleoclimatic modeling, disaster risk assessment and infrastructure maintenance (Arenson and Jakob, 2010; Colucci *et al.*, 2016; Selley *et al.*, 2018; Alcalá-Reygosa, 2019). Furthermore, the slow thawing process through heat diffusion with latent heat exchange at depth, combined with the cooling effect of the ventilated coarse blocks at the surface of rock glaciers, make them a largely inert hydrological reserve in high mountain systems (Bolch and Marchenko, 2009; Berthling, 2011; Bonnaventure and Lamoureux, 2013; Millar and Westfall, 2013). The presence and abundance of rock glaciers can therefore affect the quantities and properties of runoff from high mountain watersheds over extended time periods (Bosson and Lambiel, 2016; Jones *et al.*, 2019b).

The Tibetan Plateau (TP) is among the key high-altitude areas of periglacial landform worldwide, and is a region highly sensitive to climate change (Cui *et al.*, 2019; Yao *et al.*, 2019). Detailed rock glacier inventories have previously been constructed for the Gangdise Mountains (Zhang *et al.*, 2022), the Daxue Mountains (Ran and Liu, 2018), the Nyainqêntanglha Range (Reinosch *et al.*, 2021), and the Nepalese Himalaya (Jones *et al.*, 2018b). The Yarlung Zangbo River Basin (YZRB) is one of the regions with the highest concentrations of modern glaciers on the TP; it is experiencing the most rapid geomorphic evolution on Earth today (Ji *et al.*, 1999; Korup and Montgomery, 2008; Yu *et al.*, 2011; Long *et al.*, 2022). Although Guo (2019) characterized the spatial distribution of rock glaciers in the YZRB using manual visual interpretation, there remains a lack of any systematic and detailed rock glacier inventory, and the regional occurrence characteristics and indicative environmental significance of these rock glaciers are still unclear. Even though ground-penetrating radar (GPR), seismic refraction tomography (SRT), electrical resistivity tomography (ERT) and other geophysical techniques are widely used today and can provide new insights into understanding the ice volumes of rock glaciers and permafrost (Janke *et al*., 2015; Emmert and Kneisel, 2017; Bolch *et al*., 2019; Buckel *et al*., 2021; Halla *et al*., 2021; Mathys *et al*., 2022), it remains problematic to apply such methods to large-scale field-based research on the TP. The distribution of permafrost and the hydrological contributions made by rock glaciers on the TP need more research.

To address this, our study aims to: (i) compile a more comprehensive and systematic inventory of rock glaciers in the GLKRJ; (ii) explore the regional occurrence characteristics and indicative environmental significance of these rock glaciers; (iii) assess the regional hydrological significance of rock glaciers and clean ice glaciers; and (iv) model the distribution of the GLKRJ's permafrost probabilities.

2 Study area
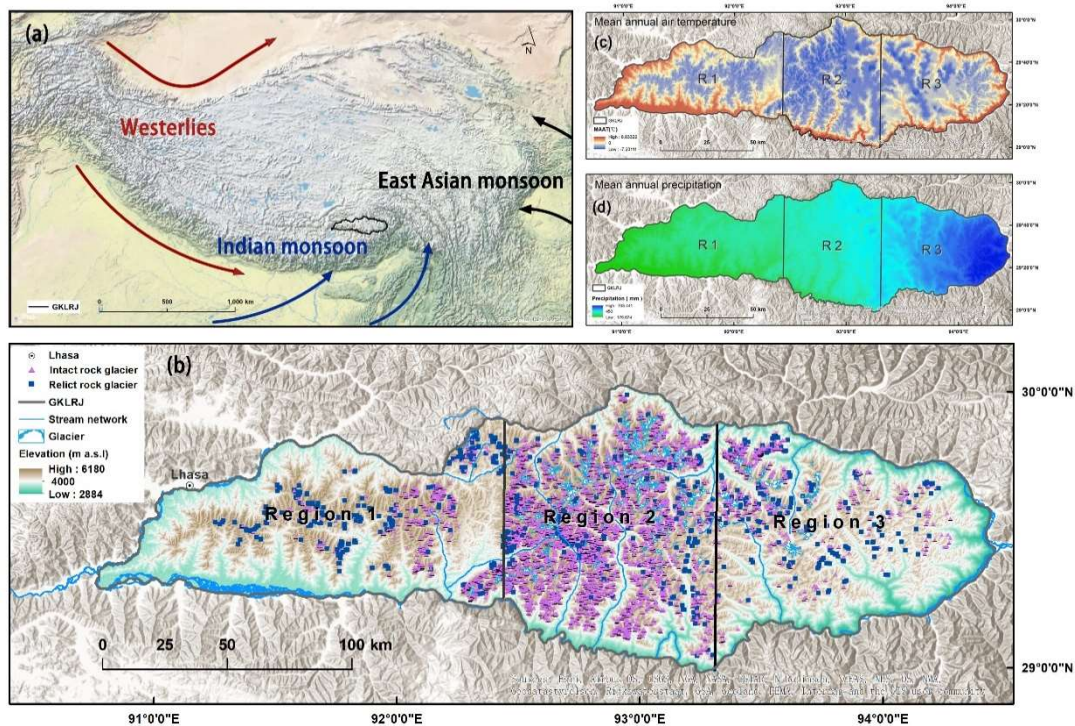
Figure 1: (a) The location of the GKLRJ on the TP; (b) The three sub-regions and the spatial distribution of streams. Rock glaciers are categorized as purple (intact rock glaciers), blue (relict rock glaciers), and glaciers are shown in blue and white; (c) Mean annual air temperature map for the GKLRJ (Du and Yi, 2019); (d) Mean annual precipitation map for the GKLRJ (Du and Yi, 2019). Maps were created using ArcGIS® software by Esri.

70

The GKLRJ region is located between 92.916°N-93.276°N and 29.287°E-29.438°E, on the southeastern TP, adjacent to the Himalayas to the south and the Nyainqêntanglha Range to the north (see Fig.1). It forms the eastern extension of the Gangdise Mountains as well as the watershed of the Yarlung Zangbo River and its tributary, the Niyang-Lhasa River, and belongs to the high mountain plateau-lake basin-wide valley area of the middle and

75 upper reaches of the Yarlung Zangbo and Nujiang rivers (Xiang *et al.*, 2013). As the GKLRJ is located in the transition belt between the TP's semi-arid and humid regions (Zheng *et al.*, 2010), it is seminal to the study of periglacial geomorphology.

Tectonically, the GKLRJ is located in the eastern part of the Ladakh-Kailas-Xiachayu magmatic arc of the Gangdise-Himalayan collisional orogen; from the Late Paleozoic to the Mesozoic, it has experienced the same

80 evolutionary tectonic processes as the Gangdise-Himalayan archipelagic arc-basin systems, *i.e.*, back-arc spreading, arc-arc collision and arc-continental collision (Pan *et al.*, 2013). The GKLRJ's main rock types include Late Cretaceous quartz monzonite, Eocene monzonite and Eocene biotite granite. Mainly dominated by the Indian Summer Monsoon (ISM), the middle and western parts of the GKLRJ belong to the TP's temperate, semi-arid zone, while the eastern part belongs to plateau's temperate humid region (Zheng *et al.*, 2010). The mean annual

85 air temperature (MAAT) is -7.2 ~ 8.8ºC (Du and Yi, 2019), and the mean annual ground temperature (MAGT) is -3.2 ~ -4.3ºC (Ran *et al.*, 2020). The mean annual precipitation (MAP) is 177-708 mm, decreasing from east to west across the study area (Du and Yi, 2019).

Table 1: Topo-climatic data for the GKLRJ and its three sub-regions.

Region	MAAT (ºC)	MAGT (ºC)	MAP (mm)	Altitude (m asl)	Mean glacier ELA (m asl)
All	0.69	0.53	469	4,623	5,431
R1	1.78	1.65	385	4,589	5,484
R2	-0.63	-0.06	489	4,893	5,462
R3	0.91	0.01	534	4,398	5,292

MAGT: mean annual ground temperature
MAAT: mean annual air temperature
MAP: mean annual precipitation

We divided the GKLRJ into three sub-regions: R1(east); R2 (central); and R3(west). These divisions were geospatially based (see Fig.1b), where R1 and R2 are bounded by the eastern marginal rift valley of the Oiga Basin, and R2 and R3 are bounded by Niang River, a tributary of the Niyang River. Each sub-region displays unique characteristics in terms of its topography and climate (see Table 1). The whole of R1 is a semi-arid region, and the terrain is more complex here. The western side of R1 is composed of a deep alpine valley landscape formed by glacial-fluvial erosion cutting through the undulating terrain, while the eastern side is a basin formed by late paleoglacial erosion and fluvial erosion cutting through less undulating mountainous hills with relatively gentle tops (Wu *et al.*, 2010). R2 is a semi-arid and semi-humid transition zone where the dividing line is located in its northeastern part; the mean altitude here is higher than in the other regions. The main peaks of glacier-carved mountains occur mostly above 5,500 m asl. R3 is located in a semi-humid zone where precipitation is more abundant and the terrain is on average ~ 500 m lower than that of R2.

3 Material and methods

3.1 Rock glacier inventory, classification and database

We used high-resolution ©Google Earth Pro remote sensing images from February 2009 to December 2020 to manually and visually interpret and compile a rock glaciers inventory for the GKLRJ (Selley *et al.*, 2018; Magori *et al.,* 2020; Hassan *et al.,* 2021). The identified rock glaciers were delineated from the rooting zone to the foot of the front slope in Google Earth Pro following the method used in previous studies (Scotti *et al.*, 2013; Jones *et al.*, 2021). The central point, length (parallel to flow) and width (vertical to flow) were also digitized in Google Earth Pro. We re-examined and adjusted the outlines of rock glaciers after the RGI_PCv2.0 (RGIK, 2022) update to ensure that they complied with the latest guidelines. Due to the lack of accurate field observations and related data on rock glacier dynamics, their activity states were determined according to the front slope, vegetation coverage, surface flow structures, rock glacier body and other geomorphic indicators. We divided rock glaciers into two types (intact/relict) according to the method used by Scotti *et al.* (2013). The active and inactive types were co-designated as 'intact rock glaciers' in this study (Haeberli, 1985; Pandey, 2019; Jones *et al.*, 2021). The intact rock glaciers usually have steep front slopes and lateral edges, an absence of vegetation cover, and apparent flow structures, such as ridges and furrows. The relict rock glaciers have relatively gentle frontal slopes, poorly defined lateral margins, a subdued topography, and less prominent flow structures (Scotti *et al.*, 2013; Baral *et al.*, 2019). Based on the sources of the sedimentary material, we divided these rock glaciers into four types: (A) intact debris-derived rock glaciers; (B) intact talus-derived rock glaciers; (C) relict debris-derived rock glaciers; and (D) relict talus-derived rock glaciers (see Fig. 2). The talus-derived rock glaciers are mostly located at the bottom of the talus slopes, and principally transport frost-shattered rock fragments derived from adjacent rock walls that

have fallen under the force of gravity. The debris-derived rock glaciers are related to perennially frozen morainic material from older glacial advances mostly between the Holocene and the Little Ice Age (LIA), and mainly transport reworked glacial debris (till) (Barsch, 1996; Lilleøren and Etzelmüller, 2011; Scotti *et al.*, 2013).
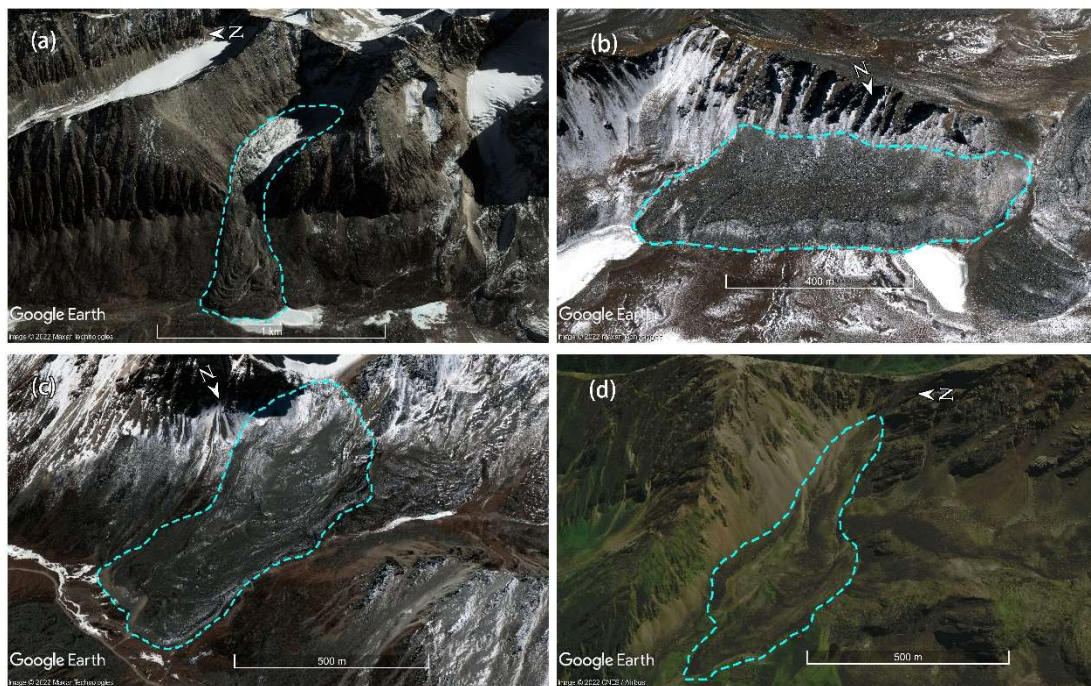
Figure 2: Example images of different types of rock glaciers in the GKLRJ. (a) An intact debris-derived rock glacier; (b) an intact talus-derived rock glacier; (c) a relict debris-derived rock glacier; (d) a relict talus-derived rock glacier. Images from ©Google Earth.

All shapefiles were fed into the 1984 UTM Zone 46N projection system to extract their topographic attributes using ArcGIS 10.7 software. The parameters (*i.e.*, latitude, longitude, area, length and width) of each rock glacier were calculated directly in ArcGIS to further divide the geometric types according to their length-width ratios. Rock glaciers with a length/width ratio of < 1 were classified as lobate-shaped rock glaciers, while those with a length/width ratio of > 1 were classified as tongue-shaped rock glaciers (Baroni *et al.*, 2004; Nyenhuis *et al.*, 2005; Scotti *et al.,* 2013). Topographic data were derived from the Terra Advanced Spaceborne Thermal Emission and Reflection Radiometer Global Digital Elevation Model Version 3 (ASTER GDEM v3). We measured the mean altitude of each rock glacier, and quantified the slope and aspect of each rock glacier using the Surface tools in the ArcGIS Spatial Analyst toolbox. Each attribute was extracted using the ArcGIS Zonal Statistics tool.

Table 2: Certainty Index applied to each rock glacier (Jones *et al*., 2018b)

Parameter	Parameter options (index code)		
	1 point	2 points	3 points
External boundary	None (ON)	Vague (OV)	Clear (OC)
Snow coverage	Snow (SS)	Partial (SP)	None (SN)
Longitudinal flow structure	None (LN)	Vague (LV)	Clear (LC)
Transverse flow structure	None (TN)	Vague (TV)	Clear (TC)
Front slope	Unclear (FU)	Gentle (FG)	Steep (FS)
Certainty Index score	Medium certainty (MC)	High certainty (HC)	Virtual certainty (VC)
	≤5	6 to 10	≥11

To reduce further the subjectivity associated with the identification, digitization and classification of landforms introduced by factors such as cloud cover, snowfall coverage and image quality in the inventory, we assessed the uncertainty for each rock glacier according to the method provided by Schmid *et al.* (2015), which has been widely used in previous studies (Jones *et al*., 2018b; Brardinoni *et al*., 2019; see Table 2). Most of the

assessment work was finished in Google Earth Pro, and we rechecked the remote sensing image in Mapcarta (https://mapcarta.com/Map) when the rock glacier was covered by snow, and without other period imagery. Finally, we recorded the certainty index of each rock glacier in the attribute table (see Supplementary Materials).

3.2 Estimating hydrological stores

To calculate more accurately the water content (water volume equivalent, WVEQ [km^3]) of intact rock glaciers and clean ice glaciers in the GKLRJ (Jones *et al.*, 2018b), we chose two different methods derived from Brenning *et al.* (2005a) and Cicoira *et al.* (2020).

The method for calculating the ice volumes of rock glaciers provided by Brenning *et al.* (2005a) requires multiplying the mean thickness, surface area and ice content of each rock glacier as in Eq. (1), then converting them to the WVEQ by assuming an ice density conversion factor of 0.9 g cm^{-3} ($\equiv$900 kg m^{-3}) (Paterson, 1994; Jones *et al.*, 2018b), thus:

$$V_{RG} = \text{Area} * \text{Mean thickness} * \text{Ice Content} \qquad (1)$$

Based on field data from Brenning *et al.* (2005a) and a rule-of-thumb given by Barsch (1977c) for the Swiss Alps, the rock glacier thickness was modeled empirically as Eq. (2), thus:

$$\text{Mean thickness [m]} = 50 * (\text{Area [km}^2\text{]})^{0.2} \qquad (2)$$

The method provided by Cicoira *et al.* (2020), based on the analysis of a dataset of 28 rock glaciers from the Alps (23) and the Andes (5), estimated rock glacier thickness using a perfectly plastic model arrived at by solving Eq. (4) for *H*, assuming a yield stress of τ = 92 kPa (taking the mean driving stress from the dataset as a given), thus:

$$H = \frac{\tau}{\rho\, g\, \sin\alpha} \pm 3.4m \qquad (3)$$

where τ is the sheer stress (τ= 92 kPa), *g* is the gravitational acceleration, *H* is the thickness of the moving rock glacier, α is the angle of the surface slope and ρ is the density of the creeping material, which is given by the contribution of volumetric debris w_d and ice content w_i and the relative densities (ρ_i = 910 kg m^{-3} and ρ_d = 2700 km m^{-3}), thus:

$$\rho = \rho_d\, w_d + \rho_i\, w_i \qquad (4)$$

Rock glaciers do not contain 100% ice by definition, and the ice content within them is spatially heterogeneous. We therefore used global estimates of ice content within rock glacier to further calculate their lower (40%), mean (50%) and upper (60%) ice volumes (Hausmann *et al.*, 2012; Krainer and Ribis, 2012; Rangecroft *et al.*, 2015; Jones *et al.*, 2018b; Wagner *et al.*, 2021). In this study, the results of the calculations that used a 50% ice content were used for subsequent comparisons with clean ice glaciers.

The ice volume of clean ice glacier was calculated using Eq. (5), thus:

$$V = A * H\,, \qquad (5)$$

where *V* represents ice volume, *A* is the glacier surface area derived from the second Chinese glacier inventory (version 1.0) (2006-2011) (Liu *et al.*, 2012), and *H* is the ice thickness calculated using GlabTop2 in Python 3.10 (Linsbauer *et al.*, 2009). We assumed a 100% ice content by volume and applied the above ice density conversion factor to calculate the water equivalent volume of clean ice glaciers.

To mitigate the additional impact caused by the uneven spatial distribution of glaciers and rock glaciers in the GKLRJ, we calculated a ratio of intact rock glaciers' to clean ice glaciers' water volume equivalence (WVEQ)

by using the weighted average method that employs the following equation:

$$\text{WVEQ ratio}_{\text{Rg: Glacier}} = \frac{\text{WVEQ R1}_{\text{Rg}} \times \frac{\text{R1}_{\text{Rg}}}{\text{All}_{\text{Rg}}} + \text{WVEQ R2}_{\text{Rg}} \times \frac{\text{R2}_{\text{Rg}}}{\text{All}_{\text{Rg}}} + \text{WVE } \text{R3}_{\text{Rg}} \times \frac{\text{R3}_{\text{Rg}}}{\text{All}_{\text{Rg}}}}{\text{WVEQ R1}_{\text{Glacier}} \times \frac{\text{R1}_{\text{Glacier}}}{\text{All}_{\text{Glacier}}} + \text{WVE } \text{R2}_{\text{Glacier}} \times \frac{\text{R2}_{\text{Glacier}}}{\text{All}_{\text{Glacier}}} + \text{WVEQ R3}_{\text{Glacier}} \times \frac{\text{R3}_{\text{Glacier}}}{\text{All}_{\text{Glacier}}}} \quad (6)$$

where WVEQ ratio$_{\text{Rg: Glacier}}$ is the ratio of intact rock glaciers' to clean ice glaciers' WEVQ; WVEQ Rn$_{\text{Rg}}$ (n = 1, 2, 3) are the WVEQ values for rock glaciers in R1, R2 and R3, respectively; Rn$_{\text{Rg}}$ (n = 1, 2, 3) are the numbers of rock glaciers in R1, R2 and R3, respectively; All$_{\text{Rg}}$ is the number of rock glaciers in the whole GKLRJ; WVEQ Rn$_{\text{Glacier}}$ (n = 1, 2, 3) are the WVEQ values for clean ice glaciers in R1, R2 and R3, respectively; Rn$_{\text{Glacier}}$ (n = 1, 2, 3) are the number of clean ice glaciers in R1, R2 and R3, respectively; and All$_{\text{Glacier}}$ is the number of clean ice glaciers in the whole GKLRJ.

3.3 Permafrost probability distribution

The binary logistic regression model has been used in several studies worldwide to calculate permafrost probability distribution (Sattler *et al.*, 2016; Deluigi *et al.*, 2017; Baral *et al.*, 2019; Hassan *et al.*, 2021). A logistic regression model can be formulated as Eq. (7), thus:

$$P(Y = 1) = \frac{1}{1 + e^{-(\beta_0 + \Sigma \beta_n X_n)}} \quad (7)$$

where $P(Y = 1)$ is the probability of outcome Y taking the value 1, β_0 is the intercept, and β_n is the regression coefficient of the independent variable X_n and is considered a predictor for the outcome Y. e is the base of the natural logarithm (Hassan *et al.*, 2021).

As viscous creep features in perennially frozen rock-ice mixtures, intact rock glaciers are considered to be direct expressions of permafrost. After calibrating the rock glacier inventory for the GKLRJ by taking activity state as the dependent variable, its intact and relict rock glaciers were taken to represent the occurrence (1) and non-occurrence (0) of permafrost, respectively. The spatially distributed local topo-climatic data (see Table 3), *i.e.*, longitude, latitude, mean altitude (ASTER GDEM v3), MAP in 2015 (Du and Yi, 2019), MAGT in 2015 (Du and Yi, 2019), mean slope and area (calculated in ArcGIS 10.7 based on ASTER GDEM v3) were used as the independent variables. All datasets were resampled to the same spatial resolution with the altitude data (~ 30 m) using the Nearest Neighbor method in ArcGIS 10.7 prior to analysis.

Table 3: Topo-climatic data information.

Factor	Year	Data source	Resolution
Latitude	/	Google Earth Pro	/
Longitude	/	Google Earth Pro	/
Area	/	ArcGIS 10.7	/
Mean altitude	2000-2013	ASTER GDEM v3	30 m
Slope	2000-2013	ASTER GDEM v3	30 m
MAGT	2005-2015	Ran *et al.,* 2019	1 km
MAP	2015	Du and Yi, 2019	1 km

MAGT: mean annual ground temperature
MAP: mean annual precipitation

We used the Forward Selection (Likelihood Ratio) method in SPSS 27.0 to stepwise select the topo-climatic variables for building the logistic regression model. The performance of the model was measured by calculating the area under the receiver operating characteristic (AUROC). A model providing excellent prediction has an AUROC higher than 0.9, a fair model has an AUROC between 0.7 and 0.9, and a model is considered poor if it has an AUROC lower than 0.7 (Swets, 1988, Marmion *et al.*, 2009).

4 Results

4.1 Rock glacier inventory

4.1.1 Rock glacier types and their distribution

We identified a total of 5,053 rock glaciers in the GKLRJ, including 830 intact debris rock glaciers (16%), 3,548 intact talus rock glaciers (70%), 68 relict debris rock glaciers (1%) and 607 relict talus rock glaciers (12%). ~ 46% of the rock glaciers were classified as lobate-shaped, and ~ 54% as tongue-shaped. Talus-derived rock glaciers are predominant in each region (Fig. 3a). However, rock glaciers are unevenly distributed in R1, R2 and R3, with nearly 70% of rock glaciers (n = 3,529) distributed in R2 (see Table 4).
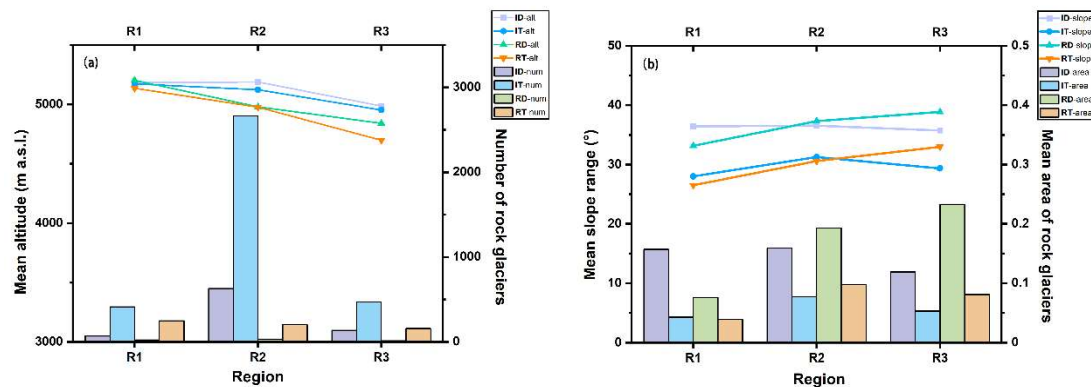
Figure 3: (a) Mean altitude and numbers of rock glaciers, by type; (b) mean range of slope and mean area of intact debris rock glaciers (ID), intact talus rock glaciers (IT), relict debris rock glaciers (RD) and relict talus rock glaciers (RT) in R1, R2 and R3.

~ 90% of the rock glaciers are located between 4,800 and 5,400 m asl, with a mean altitude of ~ 5,123 m asl. Intact rock glaciers are statistically distributed at higher altitudes than relict rock glaciers (ANOVA: F-value = 334.711, df within groups = 1, between groups = 5051, $p \leqslant 0.001$), at ~ 140 m higher. The mean altitude of rock glaciers in R1 (5,203 m asl) is higher than for those in R2 (5,189 m asl) and R3 (4,987 m asl) by ~ 40 m and ~ 250 m, respectively (see Table 4). The lower altitudinal limit of rock glaciers declines as longitude increases eastward (see Fig. 4).
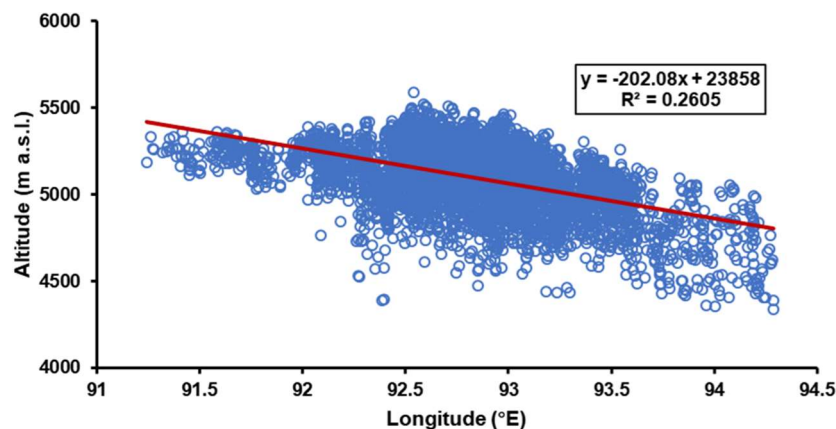
Figure 4: Scatterplots and fitted curves of the mean altitudinal distribution of rock glaciers *versus* longitude.

In the GKLRJ, rock glaciers cover an area of 428.71 km^2, with the mean area of each rock glacier being 0.08 km^2. The different types of rock glaciers vary considerably with mean area (ANOVA: F-value = 215.769, df

within groups = 3, between groups = 5049, $p \leqslant 0.001$). Debris-derived rock glaciers (0.15 km^2) generally have a larger mean area than the talus-derived ones (0.07 km^2), and relict debris rock glaciers have a larger mean area (0.16 km^2) than the other types. The mean area of most types of rock glacier is the highest in R2, except for relict debris rock glaciers, where it is smaller than in R3 (Fig. 3).

Table 4: Mean characteristics for rock glaciers.

Type	R1	R2	R3
Number	750	3,529	774
Mean altitude (m asl)	5,163	5,125	4,905
Mean MEF (m asl)	5,116	5,060	4,845
Mean area (km^3)	0.05	0.09	0.07
Mean slope range (º)	28.42	32.21	31.36
Mean MAGT (ºC)	-0.66	-0.60	-0.96
Mean MAAT (ºC)	-1.67	-1.96	-1.72
Mean MAP (mm)	339	390	502

MEF: minimum altitude at the glacier front
MAGT: mean annual ground temperature
MAAT: mean annual air temperature
MAP: mean annual precipitation

The mean range of surface slope of rock glaciers in the GKLRJ is ~ 30.46º; this value is larger than for R1 (28.42º), but smaller than for R2 (32.21º) and R3 (31.36º) (see Table 4). Moreover, debris-derived rock glaciers generally greater ranges in slope than talus-derived rock glaciers. The mean range of slope of the relict debris rock glaciers in R3 is the largest (38.87º) (Fig. 3).
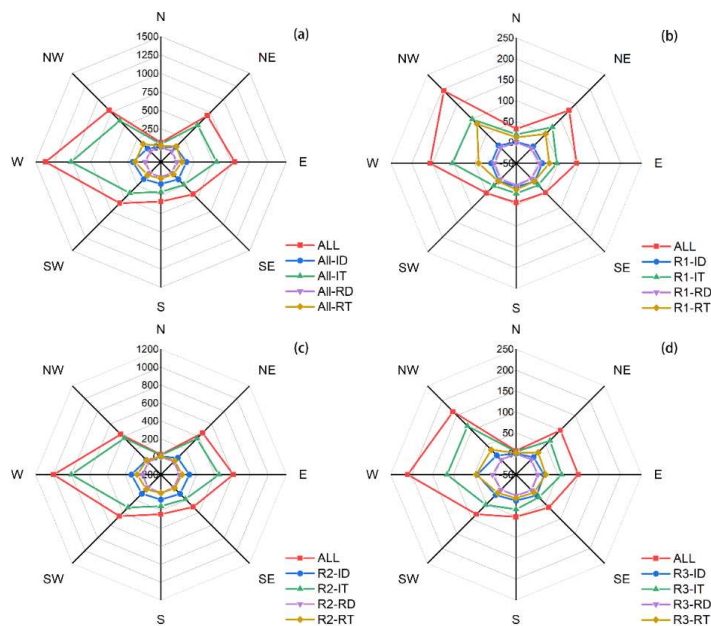
Figure 5: Analysis of abundances for different rock glacier activity states. The numbers of rock glaciers for each aspect on the four radar plots are shown as percentages (%). Note: ID = intact debris-derived rock glacier; IT = intact talus-derived rock glacier; RD = relict debris-derived rock glacier; and RT = relict talus-derived rock glacier.

Rock glaciers predominantly occur on west-facing slopes (W, 26.97%; NW, 15.69%; SW, 11.68%), with some distributed on the east-facing aspects (E, 15.85%; NE, 13.62%), and fewest on north-facing slopes (1.23%) (see Fig. 5). This is because of the existence of numerous talus rock glaciers. The numbers of rock glaciers distributed on each aspect are consistent with those for the whole study area, although the proportion of rock glaciers distributed on west-facing slopes in R1 and R3 is larger than in R2.

4.1.2 Validation of the rock glacier inventory

Nearly 90% of rock glaciers in the GKLRJ have uncertainty indices concentrated between 9 and 12. Of these, the same number of rock glaciers with uncertainty 10 and 11 (n = 1,507) account for nearly 60% of the total number of rock glaciers. In general, the numbers of rock glaciers classified as 'high certainty' (n = 2,495) and 'virtual certainty' (n = 2,558) are similar, with a relatively even spatial distribution. Intact rock glaciers generally have a high certainty index, with all of them being 'virtual certainty'. Regionally, the main factors contributing to increased uncertainty vary between regions. The rock glaciers in R1 tend to be less clear in terms of their flow structure, while those in R2 and R3 are mainly influenced by snow coverage. Furthermore, the collapsed structures of the relict rock glaciers in R3 make their surfaces much more subdued than those of intact rock glaciers.

4.2 Water equivalent volumes

Based on the second Chinese glacier inventory (Liu *et al.*, 2012), clean ice glaciers in the GKLRJ cover an area of ~ 372.32 km^2. GlabTop2 provided estimated clean ice glacier thicknesses ranging between ~ 1 and ~ 263 m (mean = ~ 18 m). We estimated the total WVEQ of the region's clean ice glaciers to be ~ 9.29 km^3.

Table 5: Ice volumes (km^3) and corresponding WVEQs (km^3) calculated using the empirical area-thickness formula (Brenning, 2005a) for sub-regions and GKLRJ-wide (All).

Region	Glacier - WVEQ (km^3)	RG - WVEQ (km^3)			RG: Glacier WVEQ ratio
		40%	50%	60%	
All	9.29	4.55	5.69	6.82	1:1.81
1	0.19	0.34	0.43	0.51	2.26:1
2	6.60	3.73	4.66	5.59	1:1.42
3	2.51	0.48	0.60	0.72	1:4.18

WVEQ = water volume equivalent

The mean ice thickness of intact rock glaciers in the GKLRJ estimated using the empirical area-thickness formula (Brenning, 2005a) is ~ 28.48 m. The WVEQ storage lies between 4.55 and 6.82 km^3, of which R2 stores ~ 80% of the water in the GKLRJ (*i.e.*, ~ 3.73-5.59 km^3). R1 stores 0.34 - 0.51 km^3 of water (8% of the whole GKLRJ reserve). R3 stores ~ 11% of the water, or 0.48 - 0.72 km^3(see Table 5). Compared to the WVEQ of clean ice glaciers, the result calculated using the weighted method showed that the ratio was 1:1.81, indicating that glaciers stored ~ 1.81 times more water than intact rock glaciers.

Table 6: Ice volumes (km^3) and corresponding WVEQs (km^3) calculated using the perfectly plastic model (Cicoira *et al.,* 2020) for sub-regions and GKLRJ-wide (All).

Region	Glacier - WVEQ (km^3)	RG - WVEQ (km^3)			RG: Glacier WVEQ ratio
		40%	50%	60%	
All	9.29	1.93 – 2.85	2.71 – 3.86	3.69 – 5.07	1:3.20
1	0.19	0.16 - 0.23	0.22 - 0.31	0.30 - 0.41	1.42:1
2	6.60	1.54 – 2.29	2.16 – 3.09	2.94 – 4.06	1:2.51
3	2.51	0.24 - 0.34	0.34 - 0.46	0.45 - 0.61	1:6.28

WVEQ = water volume equivalent
The range of results in RG - WVEQ (km^3) (Cicoira *et al.*, 2020) corresponds to $H\pm3.4$ m.

The mean thickness of rock glaciers calculated using a perfectly plastic model (Cicoira *et al.*, 2020) is 19.15±3.4 m, 9.33 m thinner than that estimated using the empirical area-thickness formula. The mean value of the WVEQ estimated using this method is ~ 56-67% of the mean value obtained using the 'Brenning' method. As

the estimated WVEQ of rock glaciers decreases, the ratio of rock glaciers' to clean ice glaciers' WVEQ is also lower than that obtained using the 'Brenning' method (Brenning, 2005a), indicating that the WVEQ of clean ice glaciers is ~ 3.2 times that of rock glaciers (see Table 6).

4.3 Logistic regression modeling of permafrost probability distribution

Table 7: Selection of dependent variables for the logistic model.

	B	SE	p	Exp(B)	BCa 95% CI(B)	
					Lower	Upper
Mean altitude	0.007	0.000	0.000	1.008	1.007	1.008
Mean annual precipitation	-0.021	0.002	0.000	0.979	0.976	0.982
Mean slope	-0.041	0.009	0.000	0.960	0.943	0.977
Mean annual ground temperature	-0.145	0.073	0.047	0.865	0.750	0.998
Area	0.000	0.000	0.016	1.000	1.000	1.000
Longitude	4.327	0.215	0.000	75.742	49.659	115.524
Latitude	-2.320	0.275	0.000	0.098	0.057	0.168
Constant	-359.428	22.036	0.000	0.000		

We generated the estimation model based the logistic regression analysis result, all coefficient of variables included in the model were highly significant ($p < 0.05$, see Table 7). The Hosmer–Lemeshow test also showed that the model was a good fit ($p = 0.709$, p > 0.05). The area under the ROC curve (AUC) was calculated to be 0.85, which suggested that the model could be reliably used to predict the GKLRJ's permafrost probability distribution.
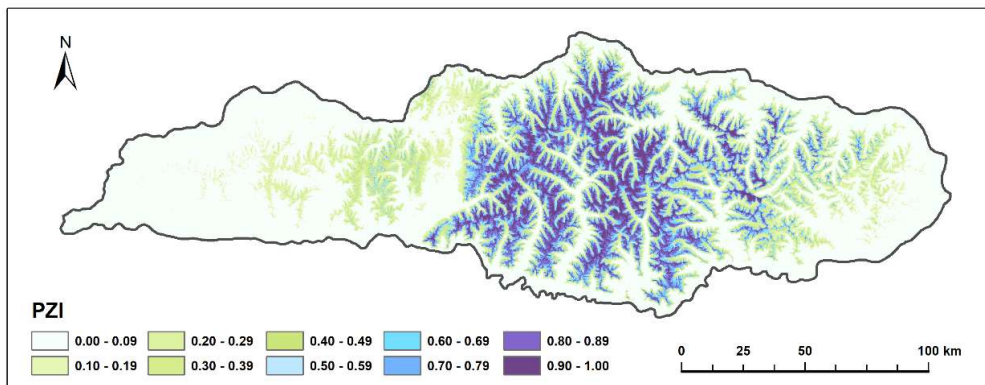
Figure 6: Permafrost probability distribution map for the GKLRJ.

Based on the above model, we drew a permafrost probability distribution map (Fig. 6). This map showed that ~ 30% of the GKLRJ (5,651 km²) is in the PZI $\geqslant$ 0.5 permafrost probability zone. The maximum area (11,708 km²; 51%) of the PZI occurs between the PZI values of 0.10 to 0.19, with a minimum altitude of 2,884 m asl, and close to the areas where MAGT = 0.5ºC and MAAT = 0ºC. The minimum altitude of permafrost probability areas with PZI values in the range of 0.50 ~ 0.59 is 4,476 m asl, where the MAGT is ~ 0ºC, close to the MAAT= -1ºC isotherm. The minimum altitude of permafrost probability areas with PZI values in the range of 0.89 ~ 0.99 is 4,790 ~ 5,860 m asl, where the MAGT is ~ -1.5ºC and the mean MAAT is ~ -3ºC, covering an area of 1,521 km² (6.6% of the total GKLRJ). As the minimum altitude of the PZI $\geqslant$ 0.5 areas is closest to the lower altitudinal limit of rock glaciers distributed in the GKLRJ (~ 4,500 m asl), we chose 0.5 as the critical value to classify the presence of permafrost in the GKLRJ. PZI $\geqslant$ 0.5 indicates that permafrost occurrence is probable, while PZI < 0.5 indicates that permafrost occurrence is improbable.

5 Discussion

5.1 Factors controlling rock glaciers distribution

Rock glaciers are distributed heterogeneously throughout the GKRLJ, with most concentrated within R2. The GKLRJ spans a large area from east to west, with variations in topography and climatic conditions between the three sub-regions, thereby providing the basis for a spatially differentiated distribution of rock glaciers. The development of rock glaciers is a complex function of responses to air temperature, insolation, wind and seasonal precipitation over a considerable time period (Humlum, 1998), with the MAAT = -2°C isotherm and the equilibrium line altitude (ELA) for local glaciers forming the lower and upper boundaries of the cryogenic belt where they have developed, respectively (Humlum, 1988; Brenning, 2005a; Rangecroft et al., 2015, 2016; Jones, 2018b). Topographically, the higher terrain in R2 has accommodated the development of more rock glaciers in the area above 4,500 m asl. R2 is located in the transition zone between the TP's semi-arid and sub-humid regions, with a mean ELA of ~ 5,462 m asl. Compared with R3, which has a lower ELA (mean ELA = 5,292 m asl), and R1, which has a higher MAAT, R2 provides a large ecological niche for rock glacier development. Additionally, the widespread glacial remains in R2 and the predominance of more easily weathered granite as bedrock in this area could also provide a richer source of material for rock glacier development (Wahrhaftig and Cox, 1959; Haeberli et al., 2006).

The mean and lower altitudinal limits of the rock glacier distribution in the GKLRJ decrease from west to east, from 5,200 m asl to ~ 4,900 m asl. In the Gangdise Mountains, located in the same latitudinal range on the western side of the study area, rock glaciers show a similar trend of gradually decreasing altitude in line with increased moisture; indeed, the characteristics of the changes in the two regions show an overall continuity (Zhang et al., 2022). Limited by the range of the ISM, MAP gradually decreases from west to east from the Gangdise Mountains to the GKLRJ. In the alpine tundra of this region, annual precipitation is dominated by snowfall in summer and autumn. Increases in snowfall in summer and autumn could help to preserve permafrost, allowing permafrost to develop at lower altitudes under similar climatic conditions (Zhou et al., 2000). Additionally, annual regional precipitation values may reflect reductions in short-wave insolation arising from cloud cover, at least to some extent (Boeckli et al., 2012a). Relatively favorable hydrological conditions will be more conducive to freeze-thaw weathering, thereby increasing the generation rate of rock debris, which in turn is conducive to the development of rock glaciers (Hallet et al., 1991; Haeberli et al., 2006; Zhang et al., 2022). Increases in MAP are therefore likely to be conducive to the expansion of the range in the distribution of rock glaciers in semi-arid to sub-humid areas, meaning that the lower altitudinal limit of rock glacier distribution decreases with increases in annual precipitation.

In the study area, rock glaciers are distributed mostly along west-facing aspects, followed by NW-facing slopes. This differs from the pattern in most regions where rock glaciers tend to be located on north-facing (NW-N-NE) mid-latitude mountains where solar radiation input is low, such as in the Himalayas (Jones et al., 2018b), Gangdise Mountains (Zhang et al., 2022), Tianshan Mountains (Liu et al., 1995; Bolch and Marchenko, 2009) and the European Alps (Scotti et al., 2013). However, regional topographic conditions appear to have a greater influence on the distribution of rock glaciers than solar radiation in the GKLRJ. The slopes here are predominantly east- and west-facing aspects, with north-facing aspects being lesson common in the region, and therefore unable to provide sufficient space for the distribution of rock glaciers. Therefore, rock glaciers within the GKLRJ are more

commonly distributed on west-facing slopes, where the potential incoming solar radiation (PISR) calculated in
SAGA 8.1.3 software is lower than for east-facing slopes.

Relict debris-derived rock glaciers exhibit a greater variation in slope within R2 and R3 compared to other types of rock glaciers. This is probably because R2 and R3 experience more intense freeze-thaw processes and more widespread glacial relics compared with R1, potentially providing a richer source of debris for rock glacier development. These debris-derived rock glaciers tend to be predominantly tongue-shaped (83%), with greater mobility and slope variation than talus-derived rock glaciers. Moreover, relict rock glaciers tend to be longer (681 m) compared to intact rock glaciers (616 m), another important factor in making their slopes more variable.

5.2 Hydrological significance of rock glaciers

In comparison, we found that the thicknesses of rock glaciers calculated using the flow plasticity model (Cicoira *et al.*, 2020) are significantly lower than the corresponding results calculated using the empirical area-thickness formula (Brenning, 2005a), potentially due to the following three main reasons. Firstly, the angle of slope used to calculate the thickness may have been overestimated. Due to the lack of actual measurement data, we calculated the length of each rock glacier in ArcGIS based on the digitized results, extracted its altitudinal difference using DEM data, and finally applied trigonometric functions to calculate each angle of slope. Secondly, the angles of slope of some rock glaciers are outside the applicable slope range of this model (10°-30°). Since tongue-shaped rock glaciers on steep hillslopes tend to have steeper slopes and greater driving stresses, our estimates of thickness using the mean parameters in the model may be lower. Thirdly, the applicability of different estimation methods may be different across the study area. The mean thickness of rock glaciers in the study made by Brenning (2005a) is ∼ 10 m higher than the sample of rock glaciers selected in the study conducted by Cicoira *et al.* (2020). The thicknesses of rock glaciers estimated using Brenning's method may therefore be overestimates.

In order to facilitate comparison with the results of different studies worldwide, we chose to use the results obtained using the empirical area-thickness formula (Brenning, 2005a) for further discussion. These estimates indicate that the amount of water stored in rock glaciers in the GKLRJ is ∼ 5.5% of the total previously-identified rock glacier water reserves globally (94.66 Gt), and ∼ 9% of the existing water reserves in rock glaciers on the TP (58.05 Gt) (Jones *et al.*, 2018a; Jones *et al.*, 2018b; Jones *et al.*, 2021). The rock glacier to glacier storage ratio in the GKJRJ of 1:1.82 is ∼ 340 times bigger than the global ratio (1:618, excluding the Antarctic and Subantarctic and Greenland Periphery Randolph Glacier Inventory) (Randolf Glacier Inventory (RGI); Pfeffer *et al.*, 2014; Jones *et al.*, 2018a), ∼ 14 times bigger than that of the Himalayas to its south (1:25) (Jones *et al.*, 2021), and much closer to that of the Andes in South America (1:3) (Azócar and Brenning, 2010), where glacier presence is also limited/absent(Schrott, 1996; Brenning, 2005b; Azócar and Brenning, 2010; Millar and Westfall, 2019; Jones *et al.*, 2019b; Schaffer *et al.*, 2019). In the GKLRJ, regional differences in the hydrological significance of rock glaciers under different climatic conditions also exist (ANOVA: *F*-value =5 8.263, df within groups = 1.773, between groups = 34.435, $p \leqslant 0.001$). In R2, which is located in the transition zone between the semi-arid and semi-humid zones, the higher topography and suitable hydrothermal conditions lead to the highest concentration of glaciers and rock glaciers in this area, with rock glaciers accounting for 82% of the rock glacier water storage in the entire study area, and glaciers accounting for ∼73% of the study area's glacial water storage, with a ratio of ∼ 1:1.42 between them. However, in terms of the ratio of rock glaciers to glacial water storage alone, rock glaciers are of greater hydrological significance in the warmer and drier R1, which has a storage capacity of only 7.6% of

the total area. In the context of drought and climate warming, rock glaciers store more than twice the water of the glaciers in R1. This partly explains why rock glaciers have a greater hydrological significance and refuge potential

390   as long-term reservoirs in arid regions with small and rapidly vanishing glaciers. Furthermore, the relationship between the proportion of the water cycle occupied by rock glaciers and the water requirements of regional populations should be considered in more detail. More research is needed into the hydrochemical composition of the stored water in rock glaciers and whether it can be used for irrigation and drinking.

5.3 Rock glaciers can be used to model permafrost probability distribution

395
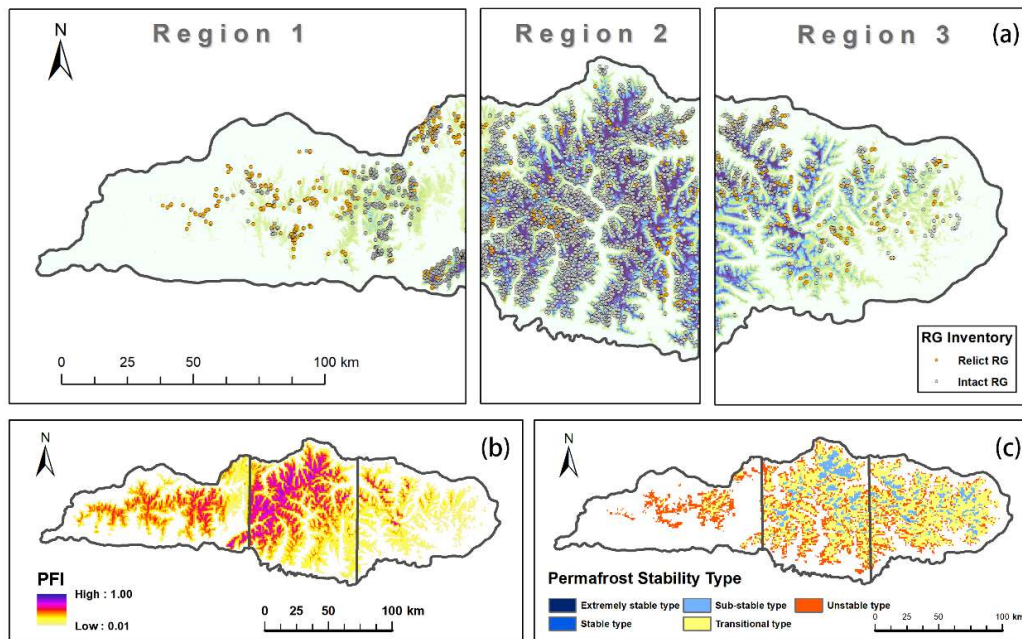
Figure 7: (a) Map of rock glaciers and permafrost probability distribution in the GKLRJ; (b) Gruber's (2012) Permafrost Zonation Index (PZI) for the GKLRJ; and (c) Map of the thermal stability of permafrost in the GKLRJ (Ran et al., 2020).

The minimum altitude at the glacier front (MEF) of the intact rock glaciers (average = ~4,500 m asl) is close to

400   the minimum altitude in the permafrost probability zone, with PZI > 0.50 (4,476 m asl), proving that the MEF of intact rock glaciers is a good indicator of permafrost distribution. Our predicted results are generally consistent with the PZI map (Gruber et al., 2012; Fig.7b) and the thermal stability of permafrost (Ran et al., 2020; Fig.7c), confirming that our rock glacier-based model has good applicability when simulating the distribution of permafrost in the GKLRJ. When making detailed comparisons between the mean MAAT data from 1961 to 1990

405   used in the study of Gruber et al. (2012) and MAAT data for the TP in 2015 provided by Du and Yi (2019), we found that, except for a few areas in the eastern part of R3, the mean MAATs of R1 and R2 increased by ~ 2ºC. Although there may have been some errors in the data, the effect of temperature on the predicted permafrost distribution for the model based on the relationship between air temperature and the occurrence of permafrost may nonetheless be somewhat magnified. These differences in the climate data's reference time periods may have

410   made our predicted range for R1 about 70% smaller than the range stated in Gruber et al. (2012). In R3, the permafrost probability distribution predicted by us is slightly lower than that of Ran et al. (2020), potentially related to the large number of relict rock glaciers in this area. Rock glaciers that extend so far from their source area, or into warmer climatic conditions at lower altitudes, may become inactive and evolve into relict rock

glaciers. In these scenarios, the probability of permafrost occurrence in the region where the rock glaciers are located may be underestimated.

6 Conclusions

We constructed an inventory of rock glaciers in the GKLRJ and illustrated their regional distribution characteristics and environmental indications. We employed two methods to estimate and compare the water storage capacity of the region's rock glaciers and map the GKLRJ's permafrost probability distribution using the binary logistic regression model. The results show that there are 5,053 rock glaciers in the GKLRJ, covering an area of 428.71 km^2. Over 80% of these rock glaciers are located within R2, and that the high altitude (~ 4,900 m asl), low temperatures (MAAT ⩽ -2ºC) and suitable precipitation (MAP ~ 400 mm) in the semi-arid and semi-humid transition zone provide the greatest ecological niche for rock glacier distribution in the region. The lower altitudinal limit of the distribution of rock glaciers decreases gradually with increasing longitude from the western side of the study area, from the Gangdise Mountains to the interior of the GKLRJ, indicating the positive effect of increased precipitation on the preservation of permafrost. Based on the empirical area-thickness formula estimation result, we calculated that 4.55-6.82 km^3 of water is stored in the rock glaciers, or ~ 61% of the water glaciers presently store. The water volume estimated on the basis of the perfectly plastic model is 56-67% of this result. Despite these differences, both of these results reveal the previously neglected and important hydrological value of rock glaciers in the GKLRJ, particularly in R1, which is the drier sub-region. The WVEQ in rock glaciers and the ratio of rock glaciers to clean ice glaciers may continue to increase with global warming and as glaciers retreat in the future. The estimated results of our regression model are in good agreement with the predictions obtained using other methods and are also consistent with the actual distribution of rock glaciers. The lower altitude of the PZI ⩾ 0.5 regions (~ 4,500 m asl) matches the boundary of the rock glacier distribution and the MAGT = 0ºC isotherm, indicating that permafrost probably occurs. This also demonstrates that our predictive approach using the rock glacier inventory can better tackle the inherent interpretive problems caused by the region's complex topographic changes, as well as reflect more accurately the GKLRJ's current permafrost probability distribution.

Data availability. The data associated with this article can be found in the Supplementary Materials. These data include the Google maps of the most important areas described in this article, as well as a tabulation of the parameters of the rock glaciers found in the GKLRJ.

Author contributions. Mengzhen Li and Gengnian Liu designed the research. Mengzhen Li performed the analysis, wrote and revised the paper. Yanmin Yang and Zhaoyu Peng provided overall supervision and gave assistance to the manuscript revision.

Competing interests. The authors declare that they have no conflict of interest.

Acknowledgments. This work was supported by the Second Tibetan Plateau Scientific Expedition and Research (STEP; Grant 299 No. 2019QZKK0205), and NSFC (Grant No. 41771005).

References

Alcalá-Reygosa, J.: Rock glaciers of the mountains of Mexico; a review of current knowledge and paleoclimatic implications, Journal of South American Earth Sciences, 96, 10.1016/j.jsames.2019.102321, 2019.

455   Arenson, L. U. and Jakob, M.: The Significance of Rock Glaciers in the Dry Andes - A Discussion of Azocar and Brenning (2010) and Brenning and Azocar (2010), Permafrost and Periglacial Processes, 21, 282-285, 10.1002/ppp.693, 2010.

Azocar, G. F. and Brenning, A.: Hydrological and Geomorphological Significance of Rock Glaciers in the Dry Andes, Chile (27 degrees-33 degrees S), Permafrost and Periglacial Processes, 21, 42-53, 10.1002/ppp.669, 2010.

460   Baral, P., Haq, M. A., and Yaragal, S.: Assessment of rock glaciers and permafrost distribution in Uttarakhand, India, Permafrost and Periglacial Processes, 31, 31-56, 10.1002/ppp.2008, 2019.

Baroni, C., Carton, A., and Seppi, R.: Distribution and behaviour of rock glaciers in the Adamello–Presanella Massif (Italian Alps), Permafrost and Periglacial Processes, 15, 243–259, https://doi.org/10.1002/ppp.497, 2004.

Barsch, D.: Permafrost creep and rock glaciers, Permafrost and Periglacial Processes, 3, 175-188, https://doi.org/10.1002/ppp.3430030303, 1992.

465   Barsch, D.: Rockglaciers: Indicators for the Present and Former Geoecology in High Mountain Environments, Springer-Verlag, Berlin, pp. 331, 10.2307/3060377, 1996.

Berthling, I.: Beyond confusion: Rock glaciers as cryo-conditioned landforms, Geomorphology, 131, 98-106, 10.1016/j.geomorph.2011.05.002, 2011.

470   Blöthe, J. H., Rosenwinkel, S., Höser, T., and Korup, O.: Rock-glacier dams in High Asia, Earth Surface Processes and Landforms, 44, 808-824, 10.1002/esp.4532, 2019.

Boeckli, L., Brenning, A., Gruber, S., and Noetzli, J.: A statistical approach to modelling permafrost distribution in the European Alps or similar mountain ranges, The Cryosphere, 6, 125-140, 10.5194/tc-6-125-2012, 2012a.

Bolch, T. and Marchenko, S.: Significance of glaciers, rockglaciers and ice-rich permafrost in the Northern Tien

475   Shan as water towers under climate change conditions, Selected Papers from the Workshop in Almaty, Kazakhstan, 2006, 8, 132–144, 2009.

Bolch, T., Rohrbach, N., Kutuzov, S., Robson, B. A., and Osmonov, A.: Occurrence, evolution and ice content of ice-debris complexes in the Ak-Shiirak, Central Tien Shan revealed by geophysical and remotely-sensed investigations, Earth Surface Processes and Landforms, 44, 129–143, https://doi.org/10.1002/esp.4487, 2019.

480   Bonnaventure, P. P. and Lamoureux, S. F.: The active layer: A conceptual review of monitoring, modelling techniques and changes in a warming climate, Progress in Physical Geography-Earth and Environment, 37, 352-376, 10.1177/0309133313478314, 2013.

Bosson, J.-B. and Lambiel, C.: Internal Structure and Current Evolution of Very Small Debris-Covered Glacier Systems Located in Alpine Permafrost Environments, Frontiers in Earth Science, 4, 10.3389/feart.2016.00039, 485   2016.

Brardinoni, F., Scotti, R., Sailer, R., and Mair, V.: Evaluating sources of uncertainty and variability in rock glacier inventories, Earth Surface Processes and Landforms, 44, 2450-2466, 10.1002/esp.4674, 2019.

Brenning, A.: Climatic and geomorphological controls of rock glaciers in the Andes of Central Chile: Combining Statistical Modelling and Field Mapping. Humboldt-Universität zu Berlin, Berlin, Germany, 2005a.

490   Brenning, A.: Geomorphological, hydrological and climatic significance of rock glaciers in the Andes of Central Chile (33-35 degrees S), Permafrost and Periglacial Processes, 16, 231-240, 10.1002/ppp.528, 2005b.

Buckel, J., Reinosch, E., Hördt, A., Zhang, F., Riedel, B., Gerke, M., Schwalb, A., and Mäusbacher, R.: Insights into a remote cryosphere: a multi-method approach to assess permafrost occurrence at the Qugaqie basin, western Nyainqêntanglha Range, Tibetan Plateau, The Cryosphere, 15, 149–168, https://doi.org/10.5194/tc-15-149-2021, 2021.

Cao, B., Li, X., Feng, M., and Zheng, D.: Quantifying Overestimated Permafrost Extent Driven by Rock Glacier Inventory, Geophysical Research Letters, 48, 10.1029/2021gl092476, 2021.

Colucci, R. R., Boccali, C., Zebre, M., and Guglielmin, M.: Rock glaciers, protalus ramparts and pronival ramparts in the south-eastern Alps, Geomorphology, 269, 112-121, 10.1016/j.geomorph.2016.06.039, 2016.

Cui, P., Guo, X., Jiang, T., Zhang, G., and Jin, W.: Disaster Effect Induced by Asian Water Tower Change and Mitigation Strategies, Bulletin of the Chinese Academy of Sciences, 34, 1313-1321, 2019.

Deluigi, N., Lambiel, C., and Kanevski, M.: Data-driven mapping of the potential mountain permafrost distribution, Science of The Total Environment, 590–591, 370–380, https://doi.org/10.1016/j.scitotenv.2017.02.041, 2017.

Du, Y. Y., Yi, J. W.: Data of climatic factors of annual mean temperature in the Xizang (1990-2015), National Tibetan Plateau Data Center [data set], 2019.

Du, Y. Y., Yi, J. W.: Data set of annual rainfall and climate factors in Tibet (1990-2015), National Tibetan Plateau Data Center [data set], 2019.

Emmert, A. and Kneisel, C.: Internal structure of two alpine rock glaciers investigated by quasi-3-D electrical resistivity imaging, The Cryosphere, 11, 841–855, https://doi.org/10.5194/tc-11-841-2017, 2017.

French, H. M.: The Periglacial Environments (3rd Ed.), John Wiley & Sons Ltd, Chichester, UK, xviii + 458 pp, 2007.

Giardino, J. R. and Vitek, J. D.: The significance of rock glaciers in the glacial-periglacial landscape continuum, Journal of Quaternary Science, 3, 97-103, https://doi.org/10.1002/jqs.3390030111, 1988.

Gruber, S.: Derivation and analysis of a high-resolution estimate of global permafrost zonation, The Cryosphere, 6, 221-233, 10.5194/tc-6-221-2012, 2012.

Guo Z: Inventorying and spatial distribution of rock glaciers in the Yarlung Zangbo River Basin, Ph.D. thesis, Institute of International Rivers and Eco-Security, Yunnan University, China, 77pp., 2019.

Haeberli, W.: Creep of Mountain Permafrost: Internal Structure and Flow of Alpine Rock Glaciers, Mitteilungen der Versuchan-stalt fur Wasserbau, Hydrologie und Glaziologie (Zürich), 77, 1985.

Haeberli, W., Hallet, B., Arenson, L., Elconin, R., Humlum, O., Kääb, A., Kaufmann, V., Ladanyi, B., Matsuoka, N., Springman, S., and Mühll, D. V.: Permafrost creep and rock glacier dynamics, Permafrost and Periglacial Processes, 17, 189-214, https://doi.org/10.1002/ppp.561, 2006.

Halla, C., Blöthe, J. H., Tapia Baldis, C., Trombotto Liaudat, D., Hilbich, C., Hauck, C., and Schrott, L.: Ice content and interannual water storage changes of an active rock glacier in the dry Andes of Argentina, The Cryosphere, 15, 1187–1213, https://doi.org/10.5194/tc-15-1187-2021, 2021.

Hassan, J., Chen, X., Muhammad, S., and Bazai, N. A.: Rock glacier inventory, permafrost probability distribution modeling and associated hazards in the Hunza River Basin, Western Karakoram, Pakistan, Sci Total Environ, 782, 146833, 10.1016/j.scitotenv.2021.146833, 2021.

530   Hausmann, H., Krainer, K., Brueckl, E., and Ullrich, C.: Internal structure, ice content and dynamics of Ölgrube and Kaiserberg rock glaciers (Ötztal Alps, Austria) determined from geophysical surveys, Austrian Journal of Earth Sciences, 105, 12-31, 2012.

Humlum, O.: Rock Glacier Appearance Level and Rock Glacier Initiation Line Altitude: A Methodological Approach to the Study of Rock Glaciers, Arctic and alpine research, 20, 160-178, 10.2307/1551495, 1988.

535   Humlum, O.: The climatic significance of rock glaciers, Permafrost and Periglacial Processes, 9, 375-395, 10.1002/(sici)1099-1530(199810/12)9:4<375::Aid-ppp301>3.0.Co;2-0, 1998.

Janke, J., Bellisario, A., and Ferrando, F.: Classification of debris-covered glaciers and rock glaciers in the Andes of central Chile, Geomorphology , 241, 98–121, https://doi.org/10.1016/j.geomorph.2015.03.034, 2015.

Ji, J.Q., Zhong, D. L., Ding, L., Zhang, J.J., and Yang, Y. C.: Genesis and scientific significance of the Yarlung

540   Zangbo Canyon, Earth Science Frontiers, 6, 231-235, 10.3321/j.issn:1005-2321.1999.04.005, 1999.

Jones, D. B., Harrison, S., Anderson, K., and Betts, R. A.: Mountain rock glaciers contain globally significant water stores, Scientific Reports, 8, 2834, 10.1038/s41598-018-21244-w, 2018a.

Jones, D. B., Harrison, S., Anderson, K., Selley, H. L., Wood, J. L., and Betts, R. A.: The distribution and hydrological significance of rock glaciers in the Nepalese Himalaya, Global and Planetary Change, 160, 123-142,

545   10.1016/j.gloplacha.2017.11.005, 2018b.

Jones, D. B., Harrison, S., Anderson, K., and Whalley, W. B.: Rock glaciers and mountain hydrology: A review, Earth-Science Reviews, 193, 66-90, 10.1016/j.earscirev.2019.04.001, 2019b.

Jones, D. B., Harrison, S., Anderson, K., Shannon, S., and Betts, R. A.: Rock glaciers represent hidden water stores in the Himalaya, Sci Total Environ, 793, 145368, 10.1016/j.scitotenv.2021.145368, 2021.

550   Kääb, A., Haeberli, W., and Gudmundsson, G. H.: Analysing the creep of mountain permafrost using high precision aerial photogrammetry: 25 years of monitoring Gruben Rock Glacier, Swiss Alps, Permafrost and Periglacial Processes, 8, 409-426, 10.1002/(sici)1099-1530(199710/12)8:4<409::Aid-ppp267>3.0.Co;2-c, 1997.

Krainer, K. and Ribis, M.: A rock glacier inventory of the Tyrolean alps (Austria), Austrian Journal of Earth Sciences, 105, 32–47, 2012.

555   Korup, O. and Montgomery, D. R.: Tibetan plateau river incision inhibited by glacial stabilization of the Tsangpo Gorge, Nature, 455, 786-U784, 10.1038/nature07322, 2008.

Lilleøren, K.S. and Etzelmüller, B.: A regional inventory of rock glaciers and ice-cored moraines in Norway, Geografiska Annaler: Series A, Physical Geography, 93, 175-191, https://doi.org/10.1111/j.1468-0459.2011.00430.x, 2011.

560   Linsbauer, A., Paul, F., Hoelzle, M., Frey, H., and Haeberli, W.: The Swiss Alps Without Glaciers - A GIS-based Modelling Approach for Reconstruction of Glacier Beds, https://doi.org/10.5167/uzh-27834, 2009.

Liu, G. N., Xiong, H. G., Cui, Z. J., and Song, C. Q.: The morphological features and environmental condition of rock glaciers in Tianshan mountains, Scientia Geographica Sinica, 15, 226-233, 297, 1995.

Liu, S., Guo, W., Xu, J.: The second glacier inventory dataset of China (version 1.0) (2006-2011). National

565   Tibetan Plateau Data Center [data set], 10.3972/glacier.001.2013.db, 2012.

Long, D., Li, X. Y., Li, X. D., Han, P. F., Zhao, F. Y., Hong, Z. K., Wang, Y. M., and Tian, F. Q.: Remote sensing retrieval of water storage changes and underlying climatic mechanisms over the Tibetan Plateau during the past two decades, Advances in Water Science, 33, 375-389, 10.14042/j.cnki.32.1309.2022.03.003, 2022.

Magori, B., Urdea, P., Onaca, A., and Ardelean, F.: Distribution and characteristics of rock glaciers in the Balkan Peninsula, Geografiska Annaler: Series A, Physical Geography, 102, 354-375, 10.1080/04353676.2020.1809905, 2020.

Mathys, T., Hilbich, C., Arenson, L. U., Wainstein, P. A., and Hauck, C.: Towards accurate quantification of ice content in permafrost of the Central Andes – Part 2: An upscaling strategy of geophysical measurements to the catchment scale at two study sites, The Cryosphere, 16, 2595–2615, https://doi.org/10.5194/tc-16-2595-2022, 2022.

Millar, C. I. and Westfall, R. D.: Rock glaciers and related periglacial landforms in the Sierra Nevada, CA, USA; inventory, distribution and climatic relationships, Quaternary International, 188, 90-104, 10.1016/j.quaint.2007.06.004, 2008.

Millar, C. I., Westfall, R. D., and Delany, D. L.: Thermal and hydrologic attributes of rock glaciers and periglacial talus landforms: Sierra Nevada, California, USA, Quaternary International, 310, 169-180, 10.1016/j.quaint.2012.07.019, 2013.

Millar, C. I. and Westfall, R. D.: Geographic, hydrological, and climatic significance of rock glaciers in the Great Basin, USA, Arctic, Antarctic, and Alpine Research, 51, 232–249, https://doi.org/10.1080/15230430.2019.1618666, 2019.

Nyenhuis, M., Hoelzle, M., and Dikau, R.: Rock glacier mapping and permafrost distribution modelling in the Turtmanntal, Valais, Switzerland, Zeitschrift fur Geomorphologie, 49, 275–292, 2005.

Pan, G. T., Wang, L. Q., Zhang, W. P., Wang, B. D.: Tectonic Map and Specification of Qinghai Tibet Plateau and Its Adjacent Areas (1: 1 500 000), Geology Press, Beijing, 208pp, 2013.

Pandey, P.: Inventory of rock glaciers in Himachal Himalaya, India using high-resolution Google Earth imagery, Geomorphology, 340, 103-115, 10.1016/j.geomorph.2019.05.001, 2019.

Paterson, W. S. B.: The Physics of Glaciers, Butterworth-Heinemann, Oxford, 480pp, 1994.

Pfeffer, W. T., Arendt, A. A., Bliss, A., Bolch, T., Cogley, J. G., Gardner, A. S., Hagen, J. O., Hock, R., Kaser, G., Kienholz, C., Miles, E. S., Moholdt, G., Mölg, N., Paul, F., Radic, V., Rastner, P., Raup, B. H., Rich, J., and Sharp, M. J.: The Randolph Glacier inventory: a globally complete inventory of glaciers, Journal of Glaciology, 60, 537-552, 2014.

Ran, Y., Li, X., Cheng, G., Nan, Z., Che, J., Sheng, Y., Wu, Q., Jin, H., Luo, D., Tang, Z., and Wu, X.: Mapping the permafrost stability on the Tibetan Plateau for 2005–2015, Science China Earth Sciences, 64, 62-79, 10.1007/s11430-020-9685-3, 2020.

Ran, Z. and Liu, G.: Rock glaciers in the Daxue Shan, south-eastern Tibetan Plateau: an inventory, their distribution, and their environmental controls, The Cryosphere, 12, 2327-2340, 10.5194/tc-12-2327-2018, 2018.

Rangecroft, S., Harrison, S., and Anderson, K.: Rock glaciers as water stores in the Bolivian Andes: an assessment of their hydrological importance, Arctic Antarctic and Alpine Research, 47, 89-98, 10.1657/aaar0014-029, 2015.

Rangecroft, S., Suggitt, A. J., Anderson, K., and Harrison, S.: Future climate warming and changes to mountain permafrost in the Bolivian Andes, Clim Change, 137, 231-243, 10.1007/s10584-016-1655-8, 2016.

Reinosch, E., Gerke, M., Riedel, B., Schwalb, A., Ye, Q., and Buckel, J.: Rock glacier inventory of the western Nyainqêntanglha Range, Tibetan Plateau, supported by InSAR time series and automated classification, Permafrost and Periglacial Processes, 32, 657-672, 10.1002/ppp.2117, 2021.

RGIK. Towards standard guidelines for inventorying rock glaciers: baseline concepts (version 4.2), IPA Action Group Rock glacier inventories and kinematics (Ed.), 13pp, 2021.

610 RGIK. Towards standard guidelines for inventorying rock glaciers: practical concepts (version 2.0). IPA Action Group Rock glacier inventories and kinematics, 10 pp. 2022.

Sattler, K., Anderson, B., Mackintosh, A., Norton, K., and de Róiste, M.: Estimating Permafrost Distribution in the Maritime Southern Alps, New Zealand, Based on Climatic Conditions at Rock Glacier Sites, Frontiers in Earth Science, 4, 10.3389/feart.2016.00004, 2016.

615 Schaffer, N., MacDonell, S., Réveillet, M., Yáñez, E., and Valois, R.: Rock glaciers as a water resource in a changing climate in the semiarid Chilean Andes, Regional Environmental Change, 19, 1263-1279, 10.1007/s10113-018-01459-3, 2019.

Schmid, M. O., Baral, P., Gruber, S., Shahi, S., Shrestha, T., Stumm, D., and Wester, P.: Assessment of permafrost distribution maps in the Hindu Kush Himalayan region using rock glaciers mapped in Google Earth, Cryosphere,

620 9, 2089-2099, 10.5194/tc-9-2089-2015, 2015.

Schrott, L.: Some geomorphological-hydrological aspects of rock glaciers in the Andes (San Juan, Argentina), Zeitschrift fur Geomorphologie, Supplementband, 104, 161–173, 1996.

Schoeneich, P., Bodin, X., Echelard, T., Kaufmann, V., Kellerer-Pirklbauer, A., Krysiecki, J.-M., and Lieb, G. K.: Velocity Changes of Rock Glaciers and Induced Hazards, in: Engineering Geology for Society and Territory -

625 Volume 1, Cham, 223–227, 2015.

Scotti, R., Brardinoni, F., Alberti, S., Frattini, P., and Crosta, G. B.: A regional inventory of rock glaciers and protalus ramparts in the central Italian Alps, Geomorphology, 186, 136-149, 10.1016/j.geomorph.2012.12.028, 2013.

Selley, H., Harrison, S., Glasser, N., Wündrich, O., Colson, D., and Hubbard, A.: Rock glaciers in central

630 Patagonia, Geografiska Annaler: Series A, Physical Geography, 101, 1-15, 10.1080/04353676.2018.1525683, 2018.

Wagner, T., Kainz, S., Helfricht, K., Fischer, A., Avian, M., Krainer, K., and Winkler, G.: Assessment of liquid and solid water storage in rock glaciers versus glacier ice in the Austrian Alps, SCIENCE OF THE TOTAL ENVIRONMENT, 800, https://doi.org/10.1016/j.scitotenv.2021.149593, 2021.

635 Wahrhaftig, C. and Cox, A.: Rock glaciers in the Alaska Range, GSA Bulletin, 70, 383-436, 10.1130/0016-7606(1959)70[383:Rgitar]2.0.Co;2, 1959.

Xiang, S. Y.: 1:3 million Quaternary geological and geomorphological map of the Tibetan Plateau and its surrounding areas, China University of Geosciences Press, Wuhan, 104pp, 2013.

Yao, T., Wu, G., Xu, B., Wang, W., Gao, J., and An, B.: Asian Water Tower Change and Its Impacts, Bulletin of

640 the Chinese Academy of Sciences, 34, 1203-1209, 2019.

Yu, X., Ji, J., Gong, J., Sun, D., Qing, J., Wang, L., Zhong, D., and Zhang, Z.: Evidence of rapid erosion driven by climate in the Yarlung Zangbo (Tsangpo) Great Canyon, the eastern Himalayan syntaxis, Chinese Science Bulletin, 56, 1123-1130, 10.1007/s11434-011-4419-x, 2011.

Zhang, Q., Jia, N., Xu, H., Yi, C., Wang, N., and Zhang, L.: Rock glaciers in the Gangdise Mountains, southern

645 Tibetan Plateau: Morphology and controlling factors, CATENA, 218, 106561, https://doi.org/10.1016/j.catena.2022.106561, 2022.

Zheng J, Yin Y, Li B. A New Scheme for Climate Regionalization in China, ACTA GEOGRAPHICA SINICA, 65, 3-12, 10.11821/xb201001002, 2010.

Zhou Y, Guo D, Qiu G, Cheng G, Li S. Geocryology In China, Science Press, Beijing, 450pp, 2000.

650